HHS Public Access

Author manuscript

*Curr Top Med Chem*. Author manuscript; available in PMC 2016 July 19.

Published in final edited form as:

*Curr Top Med Chem*. 2016 ; 16(16): 1830–1842.

# Selected PET Radioligands for Ion Channel Linked Neuroreceptor Imaging: Focus on GABA, NMDA and nACh Receptors

**Alina Kassenbrock**[1,2], **Neil Vasdev**[1,3], and **Steven H. Liang**[1,3]

[1]Division of Nuclear Medicine and Molecular Imaging, Massachusetts General Hospital, Boston, Massachusetts, USA

[2]Department of Chemistry and Chemical Biology, Northeastern University, Boston, Massachusetts, USA

[3]Department of Radiology, Harvard Medical School, Boston, Massachusetts, USA

## Abstract

Positron emission tomography (PET) neuroimaging of ion channel linked receptors is a developing area of preclinical and clinical research. The present review focuses on recent advances with radiochemistry, preclinical and clinical PET imaging studies of three receptors that are actively pursued in neuropsychiatric drug discovery: namely the γ-aminobutyric acid-benzodiazapine (GABA) receptor, nicotinic acetylcholine receptor (nAChR), and *N*-methyl-*D*-aspartate (NMDA) receptor. Recent efforts to develop new PET radioligands for these targets with improved brain uptake, selectivity, stability and pharmacokinetics are highlighted.

## Graphical abstract

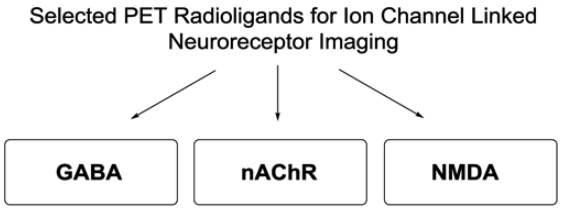


### Keywords

Positron Emission Tomography; Ion Channel; γ-Aminobutyric Acid-Benzodiazapine Receptor; Nicotinic Acetylcholine Receptor; *N*-Methyl-*D*-Aspartate Receptor

CONFLICT OF INTEREST

The authors declare no conflict of interests.

## Introduction

Positron emission tomography (PET) is a non-invasive functional imaging technique used to probe biological processes *in vivo*, via administration of radiotracers. Positron-emitting radionuclides such as carbon-11 ($^{11}C$; $t_{1/2}$ = 20.3 min) and fluorine-18 ($^{18}F$; $t_{1/2}$ = 109.7 min) decay with the emission of a positron, which subsequently annihilates upon contact with an electron to produce two 511 keV annihilation photons emitted at approximately 180° to each other.[1,2,3,4] These photons can be observed by detectors positioned in an array around the visualized object, and when both are detected simultaneously the emission event can be traced back to its location *in vivo* by analysis of the coincidence lines. In order to image a particular biological target using PET, the positron-emitting radionuclide must be "embedded" in a chemical scaffold, constituting the radiotracer (imaging probe), with the desired biological properties to both transport the radionuclide over the existing biological obstacles such as the blood brain barrier and reach the desired tissue, and interact with the molecular target of interest. PET imaging has been applied to a variety of biological processes, and can be used to diagnose and monitor the progression of numerous disease states, including cancers, cardiac disease and neurological disorders.[5] PET imaging probes can also be used to guide medicinal chemistry and drug development efforts at both preclinical and clinical stages by providing *in vivo* insights into drug binding and correlating receptor occupancy with pharmacological response. The quantitative data provided by PET is particularly useful for facilitating drug development to follow disease progression, treatment monitoring and longitudinal studies.[6]

Ion channels are membrane proteins which control the flow of ions passing through the cell membrane in almost all living species. Ion channel linked receptors are bound in cell membranes and mediated via the conformational interaction between ion channels and chemical ligands. Despite a large number of putative ion channels and related receptors proposed and identified in human genome, only few have been thoroughly studied and characterized.[7] Although PET ligand development and imaging studies in ion channel related receptors have been reviewed in the past,[8,9,10] the present review is focused on recent advances (2010 – present) with three of these receptor protein targets that we and others are interested for neuropsychiatric PET radiopharmaceutical development: the γ-aminobutyric acid-benzodiazapine (GABA) receptor, the nicotinic acetylcholine receptor (nAChR), and the *N*-methyl-D-aspartate receptor (NMDA) receptor from publications. This review highlights selected radiochemical scaffolds with emphasis on promising preclinical and clinical PET neuroimaging studies with lead tracers.

## γ-Aminobutyric Acid-Benzodiazapine Receptor

### Recent Preclinical and Clinical Research

The most commonly used PET radiotracer for imaging the γ-Aminobutyric Acid-Benzodiazapine Receptor (GABA-BZD) is radiolabeled flumazenil, an imidazo-benzodiazapine derivative which binds allosterically to the receptor.[11] This tracer can be radiolabeled with either $^{18}F$ (**Figure 1**, compound a; [$^{18}F$]flumazenil) or $^{11}C$ (**Figure 1**, compound b; [$^{11}C$]flumazenil) and an azide derivative of flumazenil, Ro15-4513 (**Figure 1**, compound c; [$^{11}C$]Ro15-4513) is also widely used. **Table 1** summarizes recent preclinical

PET imaging studies with [$^{11}$C]flumazenil, [$^{18}$F]flumazenil, or [$^{11}$C]Ro15-4513 carried out in rodents or nonhuman primates. Rodent studies were used to investigate binding and saturation of [$^{11}$C]flumazenil to the GABA receptor, and demonstrated that both receptor density and binding affinity of the tracer could be obtained in a single PET scan using a novel full saturation method.[12] [$^{11}$C]Flumazenil brain uptake was also monitored in anesthetized and awake (minimally restrained) nonhuman primates, and differences between the groups were shown to be minimal, though cortisol levels were significantly higher in awake animals.[13] Interestingly, [$^{11}$C]flumazenil brain uptake was found to be influenced by the P-glycoprotein, a blood-brain barrier brain efflux transporter, in rodents.[14]

[$^{18}$F]flumazenil was recently employed in a rat model of temporal lobe epilepsy, which elucidated a decline in hippocampal receptor density in *status epilepticus* rats when compared with healthy controls.[17] In Rhesus monkeys, socially dominant females were shown to have lower GABA receptor density in the prefrontal cortex than socially submissive animals by PET studies using [$^{18}$F]flumazenil, but administration of the corticotropin-releasing hormone astressin B to submissive females eliminated this effect.[16] [$^{11}$C]Ro15-4513 and [$^{3}$H]Ro15-4513 were used in *in vitro* studies of rat brain tissue to investigate the effects of vigabatrin, tiagabine, and SNAP-5114 on receptor agonist distribution.[18]

$^{11}$C- and $^{18}$F-labeled flumazenil have also been used extensively in clinical research studies, as summarized in **Table 2**. For instance, a significant decrease in cerebellar binding of [$^{11}$C]flumazenil was reported in three patients with cerebellar ataxia compared with healthy controls.[19] PET imaging with [$^{11}$C]flumazenil was also used to determine enhanced cognition effect of the specific GABA-α5 receptor agonist a5IA (LS-193,268) in patients without demonstrating the anxiogenic effects produced by nonspecific GABA agonists.[20] Low cerebellar binding of [$^{11}$C]flumazenil was also reported in infants with epileptic seizures.[21] Tiagibine was demonstrated to increase [$^{11}$C]flumazenil binding in a dose-dependent manner.[22] [$^{11}$C]Flumazenil PET imaging detected a decrease in GABA receptor expression and affinity in patients with primary dystonia.[23] The effectiveness of [$^{18}$F]flumazenil as a PET radiotracer was recently assessed in patients with temporal lobe epilepsy.[24] [$^{18}$F]Flumazenil imaging was used in stroke patients to monitor GABA neuroplasticity during the recovery phase, and increased GABA receptor density was correlated with the recovery of upper extremity motor function.[25] Men at ultra-high risk for psychosis showed significantly lower uptake of [$^{18}$F]flumazenil in the right caudate region of the brain.[26] Schizophrenic men taking aripiprazole had decreased [$^{18}$F]flumazenil uptake in several regions of the prefrontal cortex as compared with patients taking risperidone and healthy controls.[27] Differences in GABA receptor binding potential with [$^{18}$F]flumazenil were observed in several regions of the brain when subject awareness was directed internally verses externally.[28] [$^{18}$F]Flumazenil measurements of neuronal density were used to elucidate differences between MRI-based measurements of surface cortical thickness and actual cytoachitectonics in several brain structures.[29] [$^{11}$C]Ro15-4513 has also been used in clinical studies. This tracer was recently used to detect acute increases in synaptic GABA following the administration of tiagibine.[30] Individuals with a history of smoking showed higher distribution volume in limbic regions than nonsmokers even after a long period of

abstinence from smoking.[31] [$^{11}$C]Ro15-4513 was shown to have higher specificity for the GABA-α5 receptor subtype than flumazenil as demonstrated by dosage with the GABA-α1 selective agonist zolpidem.[32]

### Novel PET Tracers and Radiochemistry

Though the vast majority of PET imaging studies of the GABA receptor are performed with the well characterized radiotracers flumazenil and Ro15-4513, new PET ligands and radiochemistry have been reported and much of the new research focuses on the development of derivatives of the imidazo-benzodiazapine core present in both of these known tracers, with the aim to show improvement of binding affinity and radiochemical method to improve yield in a variety of ways. The synthesis of [$^{18}$F]flumazenil has been previously reported,[37] but low yields are reported and variability is high. In our experience, the synthesis of [$^{18}$F]flumazenil is complicated by the relatively large amounts of nitro-precursor (nitromazenil; **Figure 1**, compound d) required (5-10 mg) as decomposition rates compete with the radiolabeling step. An improved radiosynthesis for [$^{18}$F]flumazenil is therefore desirable.

Recent research by Jackson *et al.* focused on improving upon existing methods for the radiofluorination of flumazenil while simultaneously investigating related structures with more accessible routes of fluorination. The flumazenil derivatives were synthesized in 13-24% radiochemical yield and specific activity around 2 GBq/μmol. Eleven of these derivatives were deemed to be suitable for initial *in vivo* PET imaging studies. Two of the original compounds ([$^{18}$F]AH114726 and [$^{18}$F]GEH120348; **Figure 1**, compounds e and f) showed radiofluorination results at levels comparable with [$^{18}$F]flumazenil, and all showed improved capacity for radiofluorination.[38] A blocking study performed in rodents showed that these compounds showed tracer kinetics with similar or improved quality compared with [$^{18}$F]flumazenil. A blocking study was also carried out for the tracers in Rhesus monkey, and one compound ([$^{18}$F]AH114726) displayed pharmacodynamics similar to those of [$^{18}$F]flumazenil.[38] Though most novel radiochemistry focuses on imidazo-benzodiazapine derivatives, some have attempted to produce radioligands from other core structures. Our laboratory has focused on a novel class of tracers based on a quinoline core (**Figure 1**, compound g).[15] Two members of this class were synthesized and shown to be more selective to specific receptor subtype, i.e., $GABA_A$, than flumazenil and related benzodiazepine derivatives in *in vivo* PET imaging studies in rodents. These quinolines represent a new class of PET radiotracers for imaging the benzodiazepine site of $GABA_A$. In particular, [$^{11}$C]compound **g** readily penetrated the rat brain (>1 standard uptake value in cortical regions), had an appropriate regional brain distribution and reversible binding for $GABA_A$ receptors.

## Nicotinic Acetylcholine Receptor

Central neuronal nicotinic acetylcholine receptors are involved in various neurological process and neurodegenerative diseases, including epilepsy, depression, schizophrenia and dementia. Among all the 17 identified subtypes, α4β2-nAChR and α7-nAChR are two most prominent targets in human brain. The development of PET ligand targeting subtype α4β2

has been reviewed thoroughly[9a] and we aim to provide a brief and recent summary of preclinical and clinical use of these PET probes and recent ligand development therein.

## Recent Preclinical and Clinical Research

Several radiotracers targeting the nicotinic acetylcholine receptor (nAChR) have recently been characterized in a variety of preclinical and clinical studies (**Tables 3 and 4**). There are four PET radiotracers, namely, [$^{11}$C]nicotine, [$^{18}$F]2-FA, [$^{18}$F]6-FA and [$^{18}$F]AZAN that have been used in the imaging of α4β2 subtype in human brain.[9a] While an ideal PET ligand for this receptor has not yet been definitively established, we summarize here recent preclinical and clinical advances of PET ligands targeting nAChR, including [$^{18}$F]2-FA (**Figure 2**, compound a), [$^{18}$F]Nifene (compound b), [$^{18}$F]flubatine (compound c) and [$^{11}$C]CHIBA-1001(compound d). Specifically, [$^{18}$F]2-FA is a nicotinic acetylcholine receptor PET ligand with high affinity for the β2 subunit. The clinical applications of this tracer have recently included studies of the effects of smoking and psychiatric and degenerative disorders. PET imaging with this ligand indicated lower nAChR density in the peripheral vasculature of individuals with Parkinson's disease or multiple system atrophy.[39] A low dose of varenicline in smokers was shown by PET to fully saturate brain nAChR but had no effect on the reduction of nicotine withdrawal symptoms.[40] Tracer binding potential in the thalamus was significantly lower in paranoid schizophrenic smokers than in healthy controls.[41] Patients with Alzheimer's disease and mild cognitive impairment were demonstrated to have lower tracer binding potential than controls in regions of the brain affected by the disease.[42] [$^{18}$F]Nifene is a derivative of 2-FA with a dihydropyrrole ring (five-membered cycloamine) rather than an azetidine ring (four-membered cycloamine). This tracer has not yet been approved for clinical use but has demonstrated improved binding kinetics in preclinical studies over 2-FA, which often requires several hours to obtain a high resolution PET scan. Imaging with [$^{18}$F]nifene was used to map nAChR in the brain of rats, and a potential role for this receptor in sensory-cognitive function was evaluated.[43] Brain distribution of tracer uptake was investigated in rhesus monkeys,[44] and pharmacokinetics of the tracer was also evaluated,[45] and a blocking study was conducted.[46] [$^{18}$F]Flubatine is a nAChR PET radioligand with specificity for the α4β2 subtype.[47] This tracer was demonstrated to detect differences in synaptic acetylcholine concentration induced by receptor inhibitors in Rhesus monkeys.[48] The first fully automated radiosynthesis of this compound validated for human use[49] was reported in 2013 and first-in-human results of administration of the radiotracer showed no adverse effects in humans.[50] Tracer binding to plasma proteins in human blood was demonstrated *in vitro* and *ex vivo* to show no differences between patients with Alzheimer's disease and healthy controls.[51] [$^{11}$C]CHIBA-1001 is a PET radiotracer for the α-7 subtype of nAChR.[52] The tracer demonstrated has low specific binding for the α-7 subtype.[53] However, tracer biodistribution and kinetics have been shown to be very different in humans from the analogous rodent properties, and clinical results showed homogeneous brain uptake with low specificity.[54] Dosage with tropesitron, an α-7 receptor agonist, decreased overall brain uptake of CHIBA-1001 in humans.[55] Other radiotracers for this target include [$^{18}$F]NS-10743 (**Figure 2**, compound e), [$^{18}$F]AZAN (compound f), [$^{11}$C]NS-14492 (compound g), [$^{18}$F]nifzetidine and [$^{18}$F]ZW-104, and have been overviewed in recent publications.[56]

## Novel PET Tracers and Radiochemistry

Improvement in selectivity for the α7 subtype of the nicotinic acetylcholine receptor, which has been linked to several neurological disorders, is the focus of the majority of new radiochemistry and ligand development for this receptor. Ettrup *et al.* recently published a blocking study evaluating the *in vivo* characteristics of the nAChR α7 receptor subtype PET radioligand [$^{11}$C]NS-14492.[67] This radiotracer demonstrated high binding affinity for the target *in vitro* and high stability and selectivity *in vivo* in pigs, and was the first tracer to show dose-dependent blockade of this receptor subtype. [$^{18}$F]AZ11637326 (**Figure 2**, compound h), an α7-nAChR radioligand, was developed by Ravert *et al.*[68] This radiotracer was prepared via nucleophilic [$^{18}$F]fluorination with a subsequent decarboxylation step, resulting in about 3% overall radiochemical yield and specific activity of 140 GBq/μmol. This tracer was evaluated *in vivo* in rodents and nonhuman primates. While some level of brain uptake was observed in rodents, no specific binding was shown in nonhuman primates. Kuruvilla *et al.* developed an alternative radiotracer 2-fluoro-5-iodo-3-[2-(*S*)-3-dehydropyrrolinylmethoxy]pyridine, (**Figure 2**, compound i; [$^{18}$F]niofene) in an attempt to improve the binding kinetics of the known tracer [$^{18}$F]nifene and develop a compound suited to both PET and SPECT imaging.[69] Niofene exhibited two-fold improved binding affinity over nifene *in vitro*. In rodent PET studies, niofene showed rapid brain uptake and indicated some selectivity for the nAChR. A series of novel quinuclidine derivatives were investigated by Pin *et al.* as α7-nAChR radiotracers.[66] Amide derivatives within the series demonstrated promising *in vitro* binding results, and some of these compounds were selected for radiolabeling. One compound from the series (**Figure 2**, compound j) was evaluated in a rodent PET study and showed good penetration of the blood-brain-barrier, but also appeared to have fast clearance. [$^{18}$F]ASEM (**Figure 2**, compound k) is a radioligand developed by Gao *et. al* targeting the α7 nAChr. The original synthesis of the tracer involved substitution from a nitro derivative, resulting in 16% radiochemical yield with greater than 99% radiochemical purity and specific activity ranging from 330-1260 GBq/μmol.[62] More recently, an improved method using microwave synthesis has been reported[70] which results in 20% radiochemical yield with 856 GBq/μmol specific activity. In an initial blocking study in mice, [$^{18}$F]ASEM was demonstrated to have higher *in vivo* binding potential to the target than previously developed radioligands.[62] Specific binding to the receptor was later demonstrated to be in the range of 80-90% in baboons.[63] In a recent blocking study in healthy humans, the average binding potential of [$^{18}$F]ASEM was 10.8%.[65] Another α7 nAChR radioligand, 5-(5-(6-[$^{11}$C]methyl-3,6-diazabicyclo[3.2.0]heptan-3-yl)pyridin-2-yl)-1H-indole (**Figure 2**, compound l; [$^{11}$C]rac-(1)) was also recently developed by the same group.[71] The compound showed promising initial selectivity for the α7 receptor subtype in an *ex vivo* biodistribution study in rodents. Horti *et al.* also investigated [$^{11}$C]A-833834 (**Figure 2**, compound m) and [$^{11}$C]A-752274 (**Figure 2**, compound n), two radioligands for the α7-nAChR.[72] In PET studies in rodents, both ligands showed somewhat low brain uptake but high specificity indicated by *ex vivo* localization in the thalamus. In a nonhuman primate PET study, there was very little brain uptake of [$^{11}$C]A-752274. A new synthesis method for the nAChR radiotracer [$^{18}$F]NS14490 (**Figure 2**, compound o) proposed by Rotering *et al.* allows for the direct nucleophilic substitution of the precursor, resulting in 70% radiochemical yield.[73] This tracer demonstrated high target affinity as well as selectivity *in vitro* for the α7 receptor subtype. In rodent PET studies, low brain uptake for

the tracer was observed, but the compound had high stability in brain tissue and in plasma. [$^{18}$F]XTRA (**Figure 2**, compound p) is another radioligand developed by Gao *et. al* which targets the α4β2 nAChr (this compound was developed alongside [$^{18}$F]AZAN).[74] The original synthesis of [$^{18}$F]XTRA from a bromo precursor resulted in a radiochemical yield of 16-47%, radiochemical purity greater than 98%, and specific activity ranging from 185 GBq – 1.8TBq/μmol.[64] An improved synthetic strategy for the bromo precursor was later reported.[75] In a baboon blocking study, both [$^{18}$F]XTRA and [$^{18}$F]AZAN were demonstrated to have rapid, reversible brain kinetics.[64]

## N-methyl-D-aspartate Receptor

### Recent Clinical Research

*N*-Methyl-*D*-aspartate receptor agonists have been shown to treat symptoms of Alzheimer's disease, though no reduction in disease progression has been demonstrated. The response to NDMA receptor agonists has been monitored by PET using [$^{18}$F]FDG.[76] No PET radioligands developed for this receptor have been suitable for clinical use,[77] though it has been investigated with SPECT.[78]

### Novel PET Tracers and Radiochemistry

The *N*-methyl *D*-aspartate (NMDA) receptor is involved in neurodegenerative disease pathways, but currently has no PET-suitable radioligands available for monitoring its activity *in vivo*. Several $^{11}$C- and $^{18}$F-labeled compounds have been assessed as potential ligands, but further improvement is necessary before a satisfactory PET radiotracer is developed. Since the development of PET imaging ligand for NMDA receptor has been recently reviewed,[11] we aim to provide a brief overview of these PET probes and recent ligand development particularly after 2010. Figure 3a showed several representative NMDA ligands targeting ion channel/PCP site (CNS1261,[6, 56, 79] CNS 5161,[7, 80] GE-179[81] and GMOM[82]), glycine binding site (L-703717[83]) or NR2B subunit (MK-0657[84]). In particular, Robins *et al.* fluoroalkylated two diarylguanidine derivatives (fluoroethyl derivative is called GE-179, **Figure 3**, compound c) using thiol precursors.[85] The [$^{18}$F]fluoroalkyl compounds were prepared in 4-9% yield and up to 2.5 GBq/μmol specific activity, showing promising results regarding lipophilicity, binding affinity and selectivity for the PCP-binding site. The Sobrio research group has investigated fluoropiperidine derivatives as selective radioligands targeting NMDA receptors containing NR2B subunits. Greater brain penetration and target binding was exhibited by [$^{18}$F]*cis*-4-methylbenzyl 4-[(pyrimidin-2-ylamino)methyl]-3-fluoro-piperidine-1-carboxylate and its *trans* isomer (**Figure 3**, compound f; [$^{18}$F]MK-0567) as indicated by *ex vivo* autoradiography experiments.[86] Radiochemical yields for synthetic trials ranged from 31-45%, and the *trans* compound was produced with higher specific activity than the *cis* compound (236 vs. 170 GBq/μmol). Although $\log D_{7.4}$ values in *in vitro* assays indicated the potential for good brain penetration, low brain uptake of both $^{18}$F-isomers failed to provide satisfactory properties for imaging NMDA receptor in the living brain.[84b]

A recent example of guanidine derivative targeting NMDA NR2B subunit, PK-209, showed more than 50 fold selectivity over other targets, including adrenergic, muscarinic and opioid

receptors, as well as NMDA-PCP binding site, sigma-1 and -2, calcium and sodium ion channels. Although this tracer is metabolized rapidly in vivo, the distribution volume can be quantified in the primate brain (**Figure 3b**, compound a).[87] Two 4-(4-fluorobenzyl)piperidine compounds (**Figure 3b**, compounds b and c) were radiolabeled using nucleophilic aromatic substitution.[88] These compounds demonstrated very little brain uptake (0.035%-0.054% ID/g) in rat μPET experiments, as well as high uptake in bone tissue indicating radiodefluorination. Christiaans *et al.* recently developed a $^{11}$C-labeled radiotracer with high uptake in the rodent brain.[77] *N*-((5-(4-Fluoro-2-[$^{11}$C]methoxyphenyl)pyridin-3-yl)methyl) cyclopentanamine (**Figure 3b**, compound d) was labeled in 49% yield and 78 GBq/μmol specific activity. Rodent PET studies indicated binding to the NR2B binding site *in vivo*, but selectivity was not ideal as some binding to the sigma-1 receptor was also observed. Ametamey *et al.* demonstrated a new class of NMDA ligandm namely NB1, targeting GluN2B/NR2B subunit.[89] The autoradiography studies showed specific binding in rat brain cryosections and blocking studies demonstrated an up to 32% reduction of tracer binding, which represents a promising radiotracer for imaging NR2B subunit (**Figure 3b**, compound e). It is worthy of mention that other approaches, including NMDA SPECT agents,[90] radiolabeled drug candidate ASP0777[91], a NR2A selective radioligand [$^{18}$F]FP-PEAQX[92] and an array of candidate compounds based on CNS 1261,[93] are also disclosed in the literature in the pursue of NMDA imaging ligand.

## New Radiochemistry for PET Imaging of Other Ion Channel linked Receptor Proteins

Several noteworthy biologically active radioligands for other receptor proteins[94] have been recently reported. Specifically, investigation of chemical probes for ion channels and receptors such as the transient receptor potential vanilloid subfamily member 1 (TRPV1) receptor has yielded promising results, and a few of these results are discussed here. PET radioligands targeting TRPV1 have recently been investigated by van Veghel *et al.*[95] [$^{11}$C]DVV24 (**Figure 4**, compound a), a derivative of cinnamic acid, was obtained in up to 75% yield. This radiotracer, as well as the aminoquinazoline [$^{18}$F]DVV54 (**Figure 4**, compound b) were evaluated for biological activity in mice. Though selectivity for TRPV1 was indicated by [$^{11}$C]DVV24 retention in the trigeminal nerve, the binding affinity of both tracers was just above 100 nM, not high enough to indicate success as PET radioligands. Derivatives of *N*-(3-methoxyphenyl)-4-chlorocinnamide (**Figure 4**, compound c; [$^{11}$C]SB366791) were subsequently synthesized by van Veghel *et al.* due to the high affinity of this molecule for TRPV1. Radiochemical yield and specific activity for [$^{11}$C]SB366791 were comparable to the previous tracers, but improved *in vitro* binding affinity to both mouse (280 nM) and human (780 nM) TRPV1 was observed for this tracer. Despite these improvements, binding affinity remained low for application of this tracer to PET. The voltage gated sodium ion channels ($Na_v$s) were recently targeted for PET imaging by Hoehne *et al.*[96] $^{18}$F-radiolabeled saxitoxin (**Figure 4**, compound d) was shown to localize at the site of recent nerve injuries in rats by *in vivo* PET and *ex vivo* biodistribution studies. Tetrahydroisoquinolinium derivatives of the small conductance $Ca^{2+}$-activated $K^+$ ($SK_{Ca}$) channel blocker *N*-methyl-laudanosine (**Figure 4**, compound e) were investigated as PET radioligands of this ion channel by Gao *et al.*[97] These compounds were synthesized from

substituted isoquinoline intermediates in 40-65% yields. This series has yet to be investigated for biological activity.

## Conclusions

The GABA receptor has well-characterized PET radiotracers available for clinical research studies. The current radiochemical synthesis of [$^{18}$F]flumazenil could benefit from improvement and development of receptor subtype specific radiotracers for this target remain an ongoing area of development. Current nAChR radiotracer development focuses on improving specificity for the therapeutically relevant α7 subtype, while maintaining or improving brain uptake over known tracers. The NMDA receptor does not yet have a suitable PET radiotracer, and brain uptake remains a significant obstacle for this target. Further development still remains for satisfactory clinical PET radiotracers for ion channel linked receptors. New knowledge learned from PET imaging studies will be of importance to the design of radiopharmaceuticals for existing and new ion channel targets, and will guide neuropsychiatric and neurodegenerative drug development.

## ACKNOWLEDGEMENTS

We thank Dr. Lee Collier for helpful discussions and proofreading.

## LIST OF ABBREVIATIONS

| | |
|---|---|
| **FDG** | 2-Deoxy-2-[$^{18}$F]fluoroglucose |
| **GABA** | γ-Aminobutyric Acid-Benzodiazapine |
| **nAChR** | Nicotinic Acetylcholine Receptor |
| **$Na_vs$** | Voltage-Gated Sodium Ion Channel |
| **NMDA** | *N*-Methyl *D*-Aspartate |
| **PET** | Positron Emission Tomography |
| **$SK_{Ca}$** | Small Conductance $Ca^{2+}$-Activated $K^+$ Channel |
| **TRPV1** | Transient Receptor Potential Vanilloid Subfamily Member 1 |

## REFERENCES

1. Ametamey SM, Honer M, Schubiger PA. Molecular imaging with PET. Chem Rev. 2008; 108(5): 1501–16. [PubMed: 18426240]
2. Dolle F. Carbon-11 and fluorine-18 chemistry devoted to molecular probes for imaging the brain with positron emission tomography. Journal of labelled compounds & radiopharmaceuticals. 2013; 56(3-4):65–7. [PubMed: 24285311]
3. Cai L, Lu S, Pike VW. Chemistry with [$^{18}$F]Fluoride Ion. Eur. J. Org. Chem. 2008; 2008(17):2853–2873.
4. (a) Miller PW, Long NJ, Vilar R, Gee AD. Synthesis of $^{11}$C, $^{18}$F, $^{15}$O, and $^{13}$N radiolabels for positron emission tomography. Angew Chem Int Ed Engl. 2008; 47(47):8998–9033. [PubMed: 18988199] (b) Liang SH, Vasdev N. C(sp(3)-(18)F Bond Formation by Transition-Metal-Based [(18)F]Fluorination. Angew. Chem. Int. Ed. 2014; 53(43):11416–8.

5. Willmann JK, van Bruggen N, Dinkelborg LM, Gambhir SS. Molecular imaging in drug development. Nat Rev Drug Discov. 2008; 7(7):591–607. [PubMed: 18591980]
6. Bressan RA, Erlandsson K, Stone JM, Mulligan RS, Krystal JH, Ell PJ, Pilowsky LS. Impact of Schizophrenia and Chronic Antipsychotic Treatment on [123I]CNS-1261 Binding to N-Methyl-d-Aspartate Receptors In Vivo. Biological Psychiatry. 2005; 58(1):41–46. [PubMed: 15992521]
7. Biegon A, Gibbs A, Alvarado M, Ono M, Taylor S. In vitro and in vivo characterization of [3H]CNS-5161—A use-dependent ligand for the N-methyl-d-aspartate receptor in rat brain. Synapse. 2007; 61(8):577–586. [PubMed: 17455246]
8. (a) Andersson JD, Halldin C. PET radioligands targeting the brain GABAA /benzodiazepine receptor complex. Journal of labelled compounds & radiopharmaceuticals. 2013; 56(3-4):196–206. [PubMed: 24285326] (b) Duncan NW, Wiebking C, Northoff G. Associations of regional GABA and glutamate with intrinsic and extrinsic neural activity in humans-a review of multimodal imaging studies. Neurosci Biobehav Rev. 2014; 47:36–52. [PubMed: 25066091] (c) Deng C, Pan B, Engel M, Huang XF. Neuregulin-1 signalling and antipsychotic treatment: potential therapeutic targets in a schizophrenia candidate signalling pathway. Psychopharmacology (Berl). 2013; 226(2):201–15. [PubMed: 23389757] (d) Vogel KR, Pearl PL, Theodore WH, McCarter RC, Jakobs C, Gibson KM. Thirty years beyond discovery--clinical trials in succinic semialdehyde dehydrogenase deficiency, a disorder of GABA metabolism. J Inherit Metab Dis. 2013; 36(3):401–10. [PubMed: 22739941]
9. (a) Horti AG, Kuwabara H, Holt DP, Dannals RF, Wong DF. Recent PET radioligands with optimal brain kinetics for imaging nicotinic acetylcholine receptors. Journal of labelled compounds & radiopharmaceuticals. 2013; 56(3-4):159–66. [PubMed: 24285321] (b) Mo YX, Yin YF, Li YM. Neural nAChRs PET imaging probes. Nucl Med Commun. 2014; 35(2):135–43. [PubMed: 24240192] (c) Kober H, Deleone CM. Smoking and Neuroimaging: A Review. Curr Cardiovasc Risk Rep. 2011; 5(6):484–491. [PubMed: 24432182] (d) Wu J, Ishikawa M, Zhang J, Hashimoto K. Brain imaging of nicotinic receptors in Alzheimer's disease. Int J Alzheimers Dis. 2010; 2010:548913. [PubMed: 21253523]
10. Vlassenko AG, Benzinger TL, Morris JC. PET amyloid-beta imaging in preclinical Alzheimer's disease. Biochim Biophys Acta. 2012; 1822(3):370–9. [PubMed: 22108203]
11. (a) Fuchigami T, Nakayama M, Yoshida S. Development of PET and SPECT Probes for Glutamate Receptors. The Scientific World Journal. 2015; 2015:19.(b) Sobrio F, Gilbert G, Perrio C, Barre L, Debruyne D. PET and SPECT Imaging of the NMDA Receptor System: An Overview of Radiotracer Development. Mini Rev Med Chem. 2010; 10(9):870–886. [PubMed: 20504276] (c) Sobrio F. Radiosynthesis of carbon-11 and fluorine-18 labelled radiotracers to image the ionotropic and metabotropic glutamate receptors. Journal of Labelled Compounds and Radiopharmaceuticals. 2013; 56(3-4):180–186. [PubMed: 24285324]
12. Syvanen S, de Lange EC, Tagawa Y, Schenke M, Molthoff CF, Windhorst AD, Lammertsma AA, Voskuyl RA. Simultaneous in vivo measurements of receptor density and affinity using [$^{11}$C]flumazenil and positron emission tomography: comparison of full saturation and steady state methods. Neuroimage. 2011; 57(3):928–37. [PubMed: 21609773]
13. Sandiego CM, Jin X, Mulnix T, Fowles K, Labaree D, Ropchan J, Huang Y, Cosgrove K, Castner SA, Williams GV, Wells L, Rabiner EA, Carson RE. Awake nonhuman primate brain PET imaging with minimal head restraint: evaluation of GABAA-benzodiazepine binding with [$^{11}$C]flumazenil in awake and anesthetized animals. Journal of nuclear medicine : official publication, Society of Nuclear Medicine. 2013; 54(11):1962–8.
14. Froklage FE, Syvanen S, Hendrikse NH, Huisman MC, Molthoff CF, Tagawa Y, Reijneveld JC, Heimans JJ, Lammertsma AA, Eriksson J, de Lange EC, Voskuyl RA. [$^{11}$C]Flumazenil brain uptake is influenced by the blood-brain barrier efflux transporter P-glycoprotein. EJNMMI Res. 2012; 2:12. [PubMed: 22455873]
15. Moran MD, Wilson AA, Elmore CS, Parkes J, Ng A, Sadovski O, Graff A, Daskalakis ZJ, Houle S, Chapdelaine MJ, Vasdev N. Development of new carbon-11 labelled radiotracers for imaging GABAA- and GABAB-benzodiazepine receptors. Bioorg Med Chem. 2012; 20(14):4482–8. [PubMed: 22717238]
16. Michopoulos V, Embree M, Reding K, Sanchez MM, Toufexis D, Votaw JR, Voll RJ, Goodman MM, Rivier J, Wilson ME, Berga SL. CRH receptor antagonism reverses the effect of social

subordination upon central GABAA receptor binding in estradiol-treated ovariectomized female rhesus monkeys. Neuroscience. 2013; 250:300–8. [PubMed: 23856065]

17. Vivash L, Gregoire MC, Bouilleret V, Berard A, Wimberley C, Binns D, Roselt P, Katsifis A, Myers DE, Hicks RJ, O'Brien TJ, Dedeurwaerdere S. In vivo measurement of hippocampal GABAA/cBZR density with [$^{18}$F]-flumazenil PET for the study of disease progression in an animal model of temporal lobe epilepsy. PLoS One. 2014; 9(1):e86722. [PubMed: 24466212]
18. Quelch D, De Santis V, Strege A, Myers J, Wells L, Nutt D, Lingford-Hughes A, Parker C, Tyacke R. Influence of agonist induced internalization on [$^{3}$H]Ro15-4513 binding-an application to imaging fluctuations in endogenous GABA with positron emission tomography. Synapse. 2015; 69(1):60–5. [PubMed: 25196273]
19. Hosoi Y, Suzuki-Sakao M, Terada T, Konishi T, Ouchi Y, Miyajima H, Kono S. GABA-A receptor impairment in cerebellar ataxia with anti-glutamic acid decarboxylase antibodies. J Neurol. 2013; 260(12):3086–92. [PubMed: 24091766]
20. Eng W, Atack JR, Bergstrom M, Sanabria S, Appel L, Dawson GR, Sciberras D, Hargreaves RJ, Langstrom B, Burns HD. Occupancy of human brain GABA(A) receptors by the novel alpha5 subtype-selective benzodiazepine site inverse agonist alpha5IA as measured using [$^{11}$C]flumazenil PET imaging. Neuropharmacology. 2010; 59(7-8):635–9. [PubMed: 20696179]
21. Chugani HT, Kumar A, Muzik O. GABA(A) receptor imaging with positron emission tomography in the human newborn: a unique binding pattern. Pediatr Neurol. 2013; 48(6):459–62. [PubMed: 23668871]
22. Frankle WG, Cho RY, Mason NS, Chen CM, Himes M, Walker C, Lewis DA, Mathis CA, Narendran R. [$^{11}$C]flumazenil binding is increased in a dose-dependent manner with tiagabine-induced elevations in GABA levels. PLoS One. 2012; 7(2):e32443. [PubMed: 22384252]
23. Garibotto V, Romito LM, Elia AE, Soliveri P, Panzacchi A, Carpinelli A, Tinazzi M, Albanese A, Perani D. In vivo evidence for GABA(A) receptor changes in the sensorimotor system in primary dystonia. Mov Disord. 2011; 26(5):852–7. [PubMed: 21370265]
24. Vivash L, Gregoire MC, Lau EW, Ware RE, Binns D, Roselt P, Bouilleret V, Myers DE, Cook MJ, Hicks RJ, O'Brien TJ. [$^{18}$F]flumazenil: a gamma-aminobutyric acid A-specific PET radiotracer for the localization of drug-resistant temporal lobe epilepsy. Journal of nuclear medicine : official publication, Society of Nuclear Medicine. 2013; 54(8):1270–7.
25. Kim YK, Yang EJ, Cho K, Lim JY, Paik NJ. Functional Recovery After Ischemic Stroke Is Associated With Reduced GABAergic Inhibition in the Cerebral Cortex: A GABA PET Study. Neurorehabil Neural Repair. 2014; 28(6):576–583. [PubMed: 24463186]
26. Kang JI, Park HJ, Kim SJ, Kim KR, Lee SY, Lee E, An SK, Kwon JS, Lee JD. Reduced binding potential of GABA-A/benzodiazepine receptors in individuals at ultra-high risk for psychosis: an [$^{18}$F]-fluoroflumazenil positron emission tomography study. Schizophr Bull. 2014; 40(3):548–57. [PubMed: 23588475]
27. Lee JS, Lee JD, Park HJ, Oh MK, Chun JW, Kim SJ, Kim E, Kim JJ. Is the GABA System Related to the Social Competence Improvement Effect of Aripiprazole? An [$^{18}$F]-Fluoroflumazenil PET Study. Psychiatry Investig. 2013; 10(1):75–80.
28. Wiebking C, Duncan NW, Qin P, Hayes DJ, Lyttelton O, Gravel P, Verhaeghe J, Kostikov AP, Schirrmacher R, Reader AJ, Bajbouj M, Northoff G. External awareness and GABA--a multimodal imaging study combining fMRI and [$^{18}$F]flumazenil-PET. Hum Brain Mapp. 2014; 35(1):173–84. [PubMed: 22996793]
29. la Fougere C, Grant S, Kostikov A, Schirrmacher R, Gravel P, Schipper HM, Reader A, Evans A, Thiel A. Where in-vivo imaging meets cytoarchitectonics: the relationship between cortical thickness and neuronal density measured with high-resolution [$^{18}$F]flumazenil-PET. Neuroimage. 2011; 56(3):951–60. [PubMed: 21073964]
30. Stokes PR, Myers JF, Kalk NJ, Watson BJ, Erritzoe D, Wilson SJ, Cunningham VJ, Riano Barros D, Hammers A, Turkheimer FE, Nutt DJ, Lingford-Hughes AR. Acute increases in synaptic GABA detectable in the living human brain: a [$^{11}$C]Ro15-4513 PET study. Neuroimage. 2014; 99:158–65. [PubMed: 24844747]
31. Stokes PR, Benecke A, Myers J, Erritzoe D, Watson BJ, Kalk N, Barros DR, Hammers A, Nutt DJ, Lingford-Hughes AR. History of cigarette smoking is associated with higher limbic GABAA receptor availability. Neuroimage. 2013; 69:70–7. [PubMed: 23247185]

32. Myers JF, Rosso L, Watson BJ, Wilson SJ, Kalk NJ, Clementi N, Brooks DJ, Nutt DJ, Turkheimer FE, Lingford-Hughes AR. Characterisation of the contribution of the GABA-benzodiazepine alpha1 receptor subtype to [$^{11}$C]Ro15-4513 PET images. J Cereb Blood Flow Metab. 2012; 32(4): 731–44. [PubMed: 22214903]
33. Park HJ, Kim CH, Park ES, Park B, Oh SR, Oh MK, Park CI, Lee JD. Increased GABA-A receptor binding and reduced connectivity at the motor cortex in children with hemiplegic cerebral palsy: a multimodal investigation using [$^{18}$F]-fluoroflumazenil PET, immunohistochemistry, and MR imaging. Journal of nuclear medicine : official publication, Society of Nuclear Medicine. 2013; 54(8):1263–9.
34. Hayes DJ, Duncan NW, Wiebking C, Pietruska K, Qin P, Lang S, Gagnon J, Bing PG, Verhaeghe J, Kostikov AP, Schirrmacher R, Reader AJ, Doyon J, Rainville P, Northoff G. GABAA receptors predict aversion-related brain responses: an fMRI-PET investigation in healthy humans. Neuropsychopharmacology. 2013; 38(8):1438–50. [PubMed: 23389691]
35. Lingford-Hughes A, Reid AG, Myers J, Feeney A, Hammers A, Taylor LG, Rosso L, Turkheimer F, Brooks DJ, Grasby P, Nutt DJ. A [$^{11}$C]Ro15 4513 PET study suggests that alcohol dependence in man is associated with reduced alpha5 benzodiazepine receptors in limbic regions. J Psychopharmacol. 2012; 26(2):273–81. [PubMed: 20870689]
36. Mendez MA, Horder J, Myers J, Coghlan S, Stokes P, Erritzoe D, Howes O, Lingford-Hughes A, Murphy D, Nutt D. The brain GABA-benzodiazepine receptor alpha-5 subtype in autism spectrum disorder: a pilot [$^{11}$C]Ro15-4513 positron emission tomography study. Neuropharmacology. 2013; 68:195–201. [PubMed: 22546616]
37. (a) Odano I, Halldin C, Karlsson P, Varrone A, Airaksinen AJ, Krasikova RN, Farde L. [$^{18}$F]flumazenil binding to central benzodiazepine receptor studies by PET--quantitative analysis and comparisons with [$^{11}$C]flumazenil. Neuroimage. 2009; 45(3):891–902. [PubMed: 19136064] (b) Stephenson NA, Holland JP, Kassenbrock A, Yokell DL, Livni E, Liang SH, Vasdev N. Iodonium Ylide Mediated Radiofluorination of [$^{18}$F]FPEB and Validation for Human Use. Journal of nuclear medicine : official publication, Society of Nuclear Medicine. 2015(c) Ichiishi N, Brooks AF, Topczewski JJ, Rodnick ME, Sanford MS, Scott PJ. Copper-catalyzed [$^{18}$F]fluorination of (mesityl)(aryl)iodonium salts. Org Lett. 2014; 16(12):3224–7. [PubMed: 24890658]
38. Jackson A, Battle MR, O'Shea DM, Chau WF, Gaeta A, Brown SL, Ewan AL, Jones CL, Jones PA, Woodcraft JL, Bouvet DR, Guilbert BB, Trigg W. Evaluation of a novel series of fluorine-18-labeled imidazobenzodiazepines as potential new positron emission tomography radioligands for the GABAA receptor. Nucl Med Biol. 2014; 41(2):196–202. [PubMed: 24480268]
39. Bucerius J, Manka C, Schmaljohann J, Mani V, Gundisch D, Rudd JH, Bippus R, Mottaghy FM, Wullner U, Fayad ZA, Biersack HJ. Feasibility of [$^{18}$F]-2-Fluoro-A85380-PET imaging of human vascular nicotinic acetylcholine receptors in vivo. JACC Cardiovasc Imaging. 2012; 5(5):528–36. [PubMed: 22595161]
40. Lotfipour S, Mandelkern M, Alvarez-Estrada M, Brody AL. A single administration of low-dose varenicline saturates alpha4beta2* nicotinic acetylcholine receptors in the human brain. Neuropsychopharmacology. 2012; 37(7):1738–48. [PubMed: 22395733]
41. Brasic JR, Cascella N, Kumar A, Zhou Y, Hilton J, Raymont V, Crabb A, Guevara MR, Horti AG, Wong DF. Positron emission tomography experience with 2-[$^{18}$F]fluoro-3-(2(S)-azetidinylmethoxy)pyridine (2-[(1)(8)F]FA) in the living human brain of smokers with paranoid schizophrenia. Synapse. 2012; 66(4):352–68. [PubMed: 22169936]
42. Kendziorra K, Wolf H, Meyer PM, Barthel H, Hesse S, Becker GA, Luthardt J, Schildan A, Patt M, Sorger D, Seese A, Gertz HJ, Sabri O. Decreased cerebral alpha4beta2* nicotinic acetylcholine receptor availability in patients with mild cognitive impairment and Alzheimer's disease assessed with positron emission tomography. Eur J Nucl Med Mol Imaging. 2011; 38(3):515–25. [PubMed: 21069319]
43. Bieszczad KM, Kant R, Constantinescu CC, Pandey SK, Kawai HD, Metherate R, Weinberger NM, Mukherjee J. Nicotinic acetylcholine receptors in rat forebrain that bind [$^{18}$F]nifene: relating PET imaging, autoradiography, and behavior. Synapse. 2012; 66(5):418–34. [PubMed: 22213342]
44. Hillmer AT, Wooten DW, Slesarev MS, Ahlers EO, Barnhart TE, Schneider ML, Mukherjee J, Christian BT. Measuring alpha4beta2* nicotinic acetylcholine receptor density in vivo with

[$^{18}$F]nifene PET in the nonhuman primate. J Cereb Blood Flow Metab. 2013; 33(11):1806–14. [PubMed: 23942367]

45. Hillmer AT, Wooten DW, Moirano JM, Slesarev M, Barnhart TE, Engle JW, Nickles RJ, Murali D, Schneider ML, Mukherjee J, Christian BT. Specific alpha4beta2 nicotinic acetylcholine receptor binding of [$^{18}$F]nifene in the rhesus monkey. Synapse. 2011; 65(12):1309–18. [PubMed: 21674627]
46. Hillmer AT, Wooten DW, Slesarev MS, Ahlers EO, Barnhart TE, Murali D, Schneider ML, Mukherjee J, Christian BT. PET imaging of alpha4beta2* nicotinic acetylcholine receptors: quantitative analysis of [$^{18}$F]nifene kinetics in the nonhuman primate. Journal of nuclear medicine : official publication, Society of Nuclear Medicine. 2012; 53(9):1471–80.
47. (a) Smits R, Fischer S, Hiller A, Deuther-Conrad W, Wenzel B, Patt M, Cumming P, Steinbach J, Sabri O, Brust P, Hoepping A. Synthesis and biological evaluation of both enantiomers of [$^{18}$F]flubatine, promising radiotracers with fast kinetics for the imaging of alpha4beta2-nicotinic acetylcholine receptors. Bioorg Med Chem. 2014; 22(2):804–12. [PubMed: 24369841] (b) Fischer S, Hiller A, Smits R, Hoepping A, Funke U, Wenzel B, Cumming P, Sabri O, Steinbach J, Brust P. Radiosynthesis of racemic and enantiomerically pure (−)-[$^{18}$F]flubatine--a promising PET radiotracer for neuroimaging of alpha4beta2 nicotinic acetylcholine receptors. Appl Radiat Isot. 2013; 74:128–36. [PubMed: 23416407]
48. Gallezot JD, Esterlis I, Bois F, Zheng MQ, Lin SF, Kloczynski T, Krystal JH, Huang Y, Sabri O, Carson RE, Cosgrove KP. Evaluation of the sensitivity of the novel alpha4beta2* nicotinic acetylcholine receptor PET radioligand [$^{18}$F]-(−)-NCFHEB to increases in synaptic acetylcholine levels in rhesus monkeys. Synapse. 2014; 68(11):556–64. [PubMed: 25043426]
49. Hockley BG, Stewart MN, Sherman P, Quesada C, Kilbourn MR, Albin RL, Scott PJ. (−)-[$^{18}$F]Flubatine: evaluation in rhesus monkeys and a report of the first fully automated radiosynthesis validated for clinical use. Journal of labelled compounds & radiopharmaceuticals. 2013; 56(12):595–9. [PubMed: 24285235]
50. Sattler B, Kranz M, Starke A, Wilke S, Donat CK, Deuther-Conrad W, Patt M, Schildan A, Patt J, Smits R, Hoepping A, Schoenknecht P, Steinbach J, Brust P, Sabri O. Internal dose assessment of (−)-[$^{18}$F]flubatine, comparing animal model datasets of mice and piglets with first-in-human results. Journal of nuclear medicine : official publication, Society of Nuclear Medicine. 2014; 55(11):1885–92.
51. Patt M, Becker GA, Grossmann U, Habermann B, Schildan A, Wilke S, Deuther-Conrad W, Graef S, Fischer S, Smits R, Hoepping A, Wagenknecht G, Steinbach J, Gertz HJ, Hesse S, Schonknecht P, Brust P, Sabri O. Evaluation of metabolism, plasma protein binding and other biological parameters after administration of (−)-[$^{18}$F]Flubatine in humans. Nucl Med Biol. 2014; 41(6):489–94. [PubMed: 24768146]
52. Yin L, Zhao Q, Li L, Zhang SL, Chen XQ, Ma C, Kang L, Liu M, Zhang CL, Yan P, Wang RF. An experimental study on [$^{131}$I]CHIBA-1001: a radioligand for alpha7 nicotinic acetylcholine receptors. PLoS One. 2013; 8(7):e70188. [PubMed: 23936161]
53. Ding M, Ghanekar S, Elmore CS, Zysk JR, Werkheiser JL, Lee CM, Liu J, Chhajlani V, Maier DL. [$^{3}$H]Chiba-1001(methyl-SSR180711) has low in vitro binding affinity and poor in vivo selectivity to nicotinic alpha-7 receptor in rodent brain. Synapse. 2012; 66(4):315–22. [PubMed: 22108786]
54. Sakata M, Wu J, Toyohara J, Oda K, Ishikawa M, Ishii K, Hashimoto K, Ishiwata K. Biodistribution and radiation dosimetry of the alpha7 nicotinic acetylcholine receptor ligand [$^{11}$C]CHIBA-1001 in humans. Nucl Med Biol. 2011; 38(3):443–8. [PubMed: 21492793]
55. Ishikawa M, Sakata M, Toyohara J, Oda K, Ishii K, Wu J, Yoshida T, Iyo M, Ishiwata K, Hashimoto K. Occupancy of alpha7 Nicotinic Acetylcholine Receptors in the Brain by Tropisetron: A Positron Emission Tomography Study Using [$^{11}$C]CHIBA-1001 in Healthy Human Subjects. Clin Psychopharmacol Neurosci. 2011; 9(3):111–6. [PubMed: 23430308]
56. (a) Owens J, Tebbutt AA, McGregor AL, Kodama K, Magar SS, Perlman ME, Robins DJ, Durant GJ, McCulloch J. Synthesis and binding characteristics of N-(1-naphthyl)-N′-(3-[125I]-iodophenyl)-N′-methylguanidine ([125I]-CNS 1261): a potential SPECT agent for imaging NMDA receptor activation. Nuclear Medicine and Biology. 2000; 27(6):557–564. [PubMed: 11056369] (b) Erlandsson K, Bressan RA, Mulligan RS, Gunn RN, Cunningham VJ, Owens J,

Wyper D, Ell PJ, Pilowsky LS. Kinetic modelling of [123I]CNS 1261—a potential SPET tracer for the NMDA receptor. Nuclear Medicine and Biology. 2003; 30(4):441–454. [PubMed: 12767402]

57. Constantinescu CC, Garcia A, Mirbolooki MR, Pan ML, Mukherjee J. Evaluation of [$^{18}$F]Nifene biodistribution and dosimetry based on whole-body PET imaging of mice. Nucl Med Biol. 2013; 40(2):289–94. [PubMed: 23265670]
58. Hillmer AT, Wooten DW, Farhoud M, Higgins AT, Lao PJ, Barnhart TE, Mukherjee J, Christian BT. PET imaging of acetylcholinesterase inhibitor-induced effects on alpha4beta2 nicotinic acetylcholine receptor binding. Synapse. 2013; 67(12):882–6. [PubMed: 23913347]
59. Hillmer AT, Wooten DW, Farhoud M, Barnhart TE, Mukherjee J, Christian BT. The effects of lobeline on alpha4beta2* nicotinic acetylcholine receptor binding and uptake of [$^{18}$F]nifene in rats. J Neurosci Methods. 2013; 214(2):163–9. [PubMed: 23370310]
60. Deuther-Conrad W, Fischer S, Hiller A, Becker G, Cumming P, Xiong G, Funke U, Sabri O, Peters D, Brust P. Assessment of alpha7 nicotinic acetylcholine receptor availability in juvenile pig brain with [$^{18}$F]NS10743. Eur J Nucl Med Mol Imaging. 2011; 38(8):1541–9. [PubMed: 21484373]
61. Kuwabara H, Wong DF, Gao Y, Valentine H, Holt DP, Ravert HT, Dannals RF, Horti AG. PET Imaging of nicotinic acetylcholine receptors in baboons with [$^{18}$F]AZAN, a radioligand with improved brain kinetics. Journal of nuclear medicine : official publication, Society of Nuclear Medicine. 2012; 53(1):121–9.
62. Gao Y, Kellar KJ, Yasuda RP, Tran T, Xiao Y, Dannals RF, Horti AG. Derivatives of dibenzothiophene for positron emission tomography imaging of alpha7-nicotinic acetylcholine receptors. Journal of medicinal chemistry. 2013; 56(19):7574–89. [PubMed: 24050653]
63. Horti AG, Gao Y, Kuwabara H, Wang Y, Abazyan S, Yasuda RP, Tran T, Xiao Y, Sahibzada N, Holt DP, Kellar KJ, Pletnikov MV, Pomper MG, Wong DF, Dannals RF. [$^{18}$F]ASEM, a radiolabeled antagonist for imaging the alpha7-nicotinic acetylcholine receptor with PET. Journal of nuclear medicine : official publication, Society of Nuclear Medicine. 2014; 55(4):672–7.
64. Gao Y, Kuwabara H, Spivak CE, Xiao Y, Kellar K, Ravert HT, Kumar A, Alexander M, Hilton J, Wong DF, Dannals RF, Horti AG. Discovery of (−)-7-methyl-2-exo-[3'-(6-[$^{18}$F]fluoropyridin-2-yl)-5'-pyridinyl]-7-azabicyclo[2.2 .1]heptane, a radiolabeled antagonist for cerebral nicotinic acetylcholine receptor (alpha4beta2-nAChR) with optimal positron emission tomography imaging properties. Journal of medicinal chemistry. 2008; 51(15):4751–64. [PubMed: 18605717]
65. Wong DF, Kuwabara H, Pomper M, Holt DP, Brasic JR, George N, Frolov B, Willis W, Gao Y, Valentine H, Nandi A, Gapasin L, Dannals RF, Horti AG. Human brain imaging of alpha7 nAChR with [$^{18}$F]ASEM: a new PET radiotracer for neuropsychiatry and determination of drug occupancy. Molecular imaging and biology : MIB : the official publication of the Academy of Molecular Imaging. 2014; 16(5):730–8. [PubMed: 25145965]
66. Pin F, Vercouillie J, Ouach A, Mavel S, Gulhan Z, Chicheri G, Jarry C, Massip S, Deloye JB, Guilloteau D, Suzenet F, Chalon S, Routier S. Design of alpha7 nicotinic acetylcholine receptor ligands in quinuclidine, tropane and quinazoline series. Chemistry, molecular modeling, radiochemistry, in vitro and in rats evaluations of a [$^{18}$F]quinuclidine derivative. Eur J Med Chem. 2014; 82:214–24. [PubMed: 24904968]
67. Ettrup A, Mikkelsen JD, Lehel S, Madsen J, Nielsen EO, Palner M, Timmermann DB, Peters D, Knudsen GM. [$^{11}$C]NS14492 as a novel PET radioligand for imaging cerebral alpha7 nicotinic acetylcholine receptors: in vivo evaluation and drug occupancy measurements. Journal of nuclear medicine : official publication, Society of Nuclear Medicine. 2011; 52(9):1449–56.
68. Ravert HT, Dorff P, Foss CA, Mease RC, Fan H, Holmquist CR, Phillips E, McCarthy DJ, Heys JR, Holt DP, Wang Y, Endres CJ, Dannals RF, Pomper MG. Radiochemical synthesis and in vivo evaluation of [$^{18}$F]AZ11637326: an agonist probe for the alpha7 nicotinic acetylcholine receptor. Nucl Med Biol. 2013; 40(6):731–9. [PubMed: 23680470]
69. Kuruvilla SA, Hillmer AT, Wooten DW, Patel A, Christian BT, Mukherjee J. Synthesis and evaluation of 2-[$^{18}$F]-fluoro-5-iodo-3-[2-(S)-3,4-dehydropyrrolinylmethoxy]pyridine ((18)F-Niofene) as a potential imaging agent for nicotinic alpha4beta2 receptors. Am J Nucl Med Mol Imaging. 2014; 4(4):354–64. [PubMed: 24982821]
70. Ravert HT, Holt DP, Gao Y, Horti AG, Dannals RF. Microwave-assisted radiosynthesis of [$^{18}$F]ASEM, a radiolabeled alpha7-nicotinic acetylcholine receptor antagonist. Journal of labelled compounds & radiopharmaceuticals. 2015; 58(4):180–2. [PubMed: 25720955]

71. Gao Y, Ravert HT, Valentine H, Scheffel U, Finley P, Wong DF, Dannals RF, Horti AG. 5-(5-(6-[$^{11}$C]methyl-3,6-diazabicyclo[3.2.0]heptan-3-yl)pyridin-2-yl)-1H-indole as a potential PET radioligand for imaging cerebral alpha7-nAChR in mice. Bioorg Med Chem. 2012; 20(12):3698–702. [PubMed: 22608919]
72. Horti AG, Ravert HT, Gao Y, Holt DP, Bunnelle WH, Schrimpf MR, Li T, Ji J, Valentine H, Scheffel U, Kuwabara H, Wong DF, Dannals RF. Synthesis and evaluation of new radioligands [$^{11}$C]A-833834 and [$^{11}$C]A-752274 for positron-emission tomography of alpha7-nicotinic acetylcholine receptors. Nucl Med Biol. 2013; 40(3):395–402. [PubMed: 23294899]
73. Rotering S, Scheunemann M, Fischer S, Hiller A, Peters D, Deuther-Conrad W, Brust P. Radiosynthesis and first evaluation in mice of [$^{18}$F]NS14490 for molecular imaging of alpha7 nicotinic acetylcholine receptors. Bioorg Med Chem. 2013; 21(9):2635–42. [PubMed: 23507153]
74. Horti AG, Gao Y, Kuwabara H, Dannals RF. Development of radioligands with optimized imaging properties for quantification of nicotinic acetylcholine receptors by positron emission tomography. Life sciences. 2010; 86(15-16):575–84. [PubMed: 19303028]
75. Gao Y, Wang H, Mease RC, Pomper MG, Horti AG. Improved Syntheses of Precursors for PET Radioligands [$^{18}$F]XTRA and [$^{18}$F]AZAN. Tetrahedron letters. 2010; 51(40):5333–5335. [PubMed: 20835363]
76. Shirakawa T, Mitsuoka K, Kuroda K, Miyoshi S, Shiraki K, Naraoka H, Noda A, Fujikawa A, Fujiwara M. [$^{18}$F]FDG-PET as an imaging biomarker to NMDA receptor antagonist-induced neurotoxicity. Toxicol Sci. 2013; 133(1):13–21. [PubMed: 23457119]
77. Christiaans JA, Klein PJ, Metaxas A, Kooijman EJ, Schuit RC, Leysen JE, Lammertsma AA, van Berckel BN, Windhorst AD. Synthesis and preclinical evaluation of carbon-11 labelled N-((5-(4-fluoro-2-[$^{11}$C]methoxyphenyl)pyridin-3-yl)methyl)cyclopentanamine as a PET tracer for NR2B subunit-containing NMDA receptors. Nucl Med Biol. 2014; 41(8):670–80. [PubMed: 24929961]
78. Sasmal DK, Lu HP. Single-molecule patch-clamp FRET microscopy studies of NMDA receptor ion channel dynamics in living cells: revealing the multiple conformational states associated with a channel at its electrical off state. J Am Chem Soc. 2014; 136(37):12998–3005. [PubMed: 25148304]
79. Bressan RA, Erlandsson K, Mulligan RS, Gunn RN, Cunningham VJ, Owens J, Cullum ID, Ell PJ, Pilowsky LS. A bolus/infusion paradigm for the novel NMDA receptor SPET tracer [123i]CNS 1261. Nuclear Medicine and Biology. 2004; 31(2):155–164. [PubMed: 15013480]
80. Dhawan V, Robeson W, Bjelke D, Chaly T, Graf K, Hellman M, Zhuo L, Mackay M, Eidelberg D. Human Radiation Dosimetry for the N-Methyl-d-Aspartate Receptor Radioligand 11C-CNS5161. Journal of Nuclear Medicine. 2015; 56(6):869–872. [PubMed: 25931480]
81. (a) Robins EG, Zhao Y, Khan I, Wilson A, Luthra SK, Årstad E. Synthesis and in vitro evaluation of 18F-labelled S-fluoroalkyl diarylguanidines: Novel high-affinity NMDA receptor antagonists for imaging with PET. Bioorganic & Medicinal Chemistry Letters. 2010; 20(5):1749–1751. [PubMed: 20138515] (b) McGinnity CJ, Hammers A, Riaño Barros DA, Luthra SK, Jones PA, Trigg W, Micallef C, Symms MR, Brooks DJ, Koepp MJ, Duncan JS. Initial Evaluation of 18F-GE-179, a Putative PET Tracer for Activated N-Methyl d-Aspartate Receptors. Journal of Nuclear Medicine. 2014; 55(3):423–430. [PubMed: 24525206]
82. (a) Waterhouse RN, Slifstein M, Dumont F, Zhao J, Chang RC, Sudo Y, Sultana A, Balter A, Laruelle M. In vivo evaluation of [11C]N-(2-chloro-5-thiomethylphenyl)-N′- (3-methoxy-phenyl)-N′-methylguanidine ([11C]GMOM) as a potential PET radiotracer for the PCP/NMDA receptor. Nuclear Medicine and Biology. 2004; 31(7):939–948. [PubMed: 15464396] (b) Golla S, van der Doef T, Oropeza Seguias G, Bakker E, Klein P, Schuit R, Windhorst A, Lammertsma A, Van Berckel B, Boellaard R. Kinetic analysis of the NMDA receptor ligand [11C]GMOM in men. Journal of Nuclear Medicine. 2014; 55(supplement 1):2027.
83. (a) Haradahira T, Zhang M-R, Maeda J, Okauchi T, Kawabe K, Kida T, Suzuki K, Suhara T. A strategy for increasing the brain uptake of a radioligand in animals: use of a drug that inhibits plasma protein binding. Nuclear Medicine and Biology. 2000; 27(4):357–360. [PubMed: 10938470] (b) Haradahira T, Okauchi T, Maeda J, Zhang M-R, Nishikawa T, Konno R, Suzuki K, Suhara T. Effects of endogenous agonists, glycine and D-serine, on in vivo specific binding of [11C]L-703,717, a PET radioligand for the glycine-binding site of NMDA receptors. Synapse. 2003; 50(2):130–136. [PubMed: 12923815] (c) Haradahira T, Zhang M-R, Maeda J, Okauchi T,

Kida T, Kawabe K, Sasaki S, Suhara T, Suzuki K. A Prodrug of NMDA/Glycine Site Antagonist, L-703, 717, with Improved BBB Permeability: 4-Acetoxy Derivative and Its Positron-Emitter Labeled Analog. Chemical and Pharmaceutical Bulletin. 2001; 49(2):147–150. [PubMed: 11217099]

84. (a) Koudih R, Gilbert G, Dhilly M, Abbas A, Barré L, Debruyne D, Sobrio F. Synthesis and in vitro characterization of trans- and cis-[18F]-4-methylbenzyl 4-[(pyrimidin-2-ylamino)methyl]-3-fluoropiperidine-1-carboxylates as new potential PET radiotracer candidates for the NR2B subtype N-methyl-d-aspartate receptor. European Journal of Medicinal Chemistry. 2012; 53:408–415. [PubMed: 22554495] (b) Koudih R, Gilbert G, Dhilly M, Abbas A, Barre L, Debruyne D, Sobrio F. Radiolabelling of 1,4-disubstituted 3-[18F]fluoropiperidines and its application to new radiotracers for NR2B NMDA receptor visualization. Organic & Biomolecular Chemistry. 2012; 10(42):8493–8500. [PubMed: 23007637]

85. Robins EG, Zhao Y, Khan I, Wilson A, Luthra SK, Rstad E. Synthesis and in vitro evaluation of $^{18}$F-labelled S-fluoroalkyl diarylguanidines: Novel high-affinity NMDA receptor antagonists for imaging with PET. Bioorg Med Chem Lett. 2010; 20(5):1749–51. [PubMed: 20138515]

86. Koudih R, Gilbert G, Dhilly M, Abbas A, Barre L, Debruyne D, Sobrio F. Synthesis and in vitro characterization of trans- and cis-[$^{18}$F]-4-methylbenzyl 4-[(pyrimidin-2-ylamino)methyl]-3-fluoropiperidine-1-carboxylates as new potential PET radiotracer candidates for the NR2B subtype N-methyl-D-aspartate receptor. Eur J Med Chem. 2012; 53:408–15. [PubMed: 22554495]

87. Golla SSV, Klein PJ, Bakker J, Schuit RC, Christiaans JAM, van Geest L, Kooijman EJM, Oropeza-Seguias GM, Langermans JAM, Leysen JE, Boellaard R, Windhorst AD, van Berckel BNM, Metaxas A. Preclinical evaluation of [18F]PK-209, a new PET ligand for imaging the ion-channel site of NMDA receptors. Nuclear Medicine and Biology. 2015; 42(2):205–212. [PubMed: 25451213]

88. Labas R, Gilbert G, Nicole O, Dhilly M, Abbas A, Tirel O, Buisson A, Henry J, Barre L, Debruyne D, Sobrio F. Synthesis, evaluation and metabolic studies of radiotracers containing a 4-(4-[$^{18}$F]-fluorobenzyl)piperidin-1-yl moiety for the PET imaging of NR2B NMDA receptors. Eur J Med Chem. 2011; 46(6):2295–309. [PubMed: 21453995]

89. Betzel T, Tewes B, Frehland B, Schepmann D, Krämer SD, Schibli R, Wünsch B, Ametamey SM. Development of a PET Ligand for Imaging GluN2B Subunit of the NMDA Receptor. Journal of Labelled Compounds and Radiopharmaceuticals. 2015; 58:S41.

90. (a) Fuchigami T, Yamaguchi H, Ogawa M, Biao L, Nakayama M, Haratake M, Magata Y. Synthesis and biological evaluation of radio-iodinated benzimidazoles as SPECT imaging agents for NR2B subtype of NMDA receptor. Bioorganic & Medicinal Chemistry. 2010; 18(21):7497–7506. [PubMed: 20875744] (b) Zhou X, Zhang J, Yan C, Cao G, Zhang R, Cai G, Jiang M, Wang S. Preliminary studies of 99mTc-memantine derivatives for NMDA receptor imaging. Nuclear Medicine and Biology. 2012; 39(7):1034–1041. [PubMed: 22516779]

91. Noda A, Murakami Y, Miyoshi S, Nishimura S. Macaque brain PET study on [11C]ASP0777, an non-competitive NMDA receptor antagonist. Journal of Nuclear Medicine. 2014; 55(supplement 1):1816.

92. Sephton SM, Auberson Y, Cermak S, Mu L, Herde AM, Schibli R, Krämer SD, Ametamey SM. Radiosynthesis and In Vitro Evaluation of [$^{18}$F]FP-PEAQX as a Potential PET Radioligand for Imaging the GluN2A Subunit of the NMDA Receptor. Journal of Labelled Compounds and Radiopharmaceuticals. 2015; 58:S410.

93. Naumiec GR, Cai L, Pike VW. New N-aryl-N′-(3-(substituted)phenyl)-N′-methylguanidines as leads to potential PET radioligands for imaging the open NMDA receptor. Bioorganic & Medicinal Chemistry Letters. 2015; 25(2):225–228. [PubMed: 25499436]

94. Sobrio F. Radiosynthesis of carbon-11 and fluorine-18 labelled radiotracers to image the ionotropic and metabotropic glutamate receptors. Journal of labelled compounds & radiopharmaceuticals. 2013; 56(3-4):180–6. [PubMed: 24285324]

95. (a) van Veghel D, Cleynhens J, Pearce LV, Blumberg PM, Van Laere K, Verbruggen A, Bormans G. Synthesis and biological evaluation of [$^{11}$C]SB366791: a new PET-radioligand for in vivo imaging of the TRPV1 receptor. Nucl Med Biol. 2013; 40(1):141–7. [PubMed: 23141549] (b) van Veghel D, Cleynhens J, Pearce LV, DeAndrea-Lazarus IA, Blumberg PM, Van Laere K, Verbruggen A, Bormans G. New transient receptor potential vanilloid subfamily member 1 positron emission

tomography radioligands: synthesis, radiolabeling, and preclinical evaluation. ACS Chem Neurosci. 2013; 4(4):624–34. [PubMed: 23421633]

96. Hoehne A, Behera D, Parsons WH, James ML, Shen B, Borgohain P, Bodapati D, Prabhakar A, Gambhir SS, Yeomans DC, Biswal S, Chin FT, Du Bois J. A 18F-labeled saxitoxin derivative for in vivo PET-MR imaging of voltage-gated sodium channel expression following nerve injury. J Am Chem Soc. 2013; 135(48):18012–5. [PubMed: 24261833]
97. Gao M, Wang M, Zheng QH. Synthesis of carbon-11 labeled 1-(3,4-dimethoxybenzyl)-2,2-dimethyl-1,2,3,4-tetrahydroisoquinolinium derivatives as new potential PET SKCa channel imaging agents. Appl Radiat Isot. 2008; 66(2):194–202. [PubMed: 17905592]

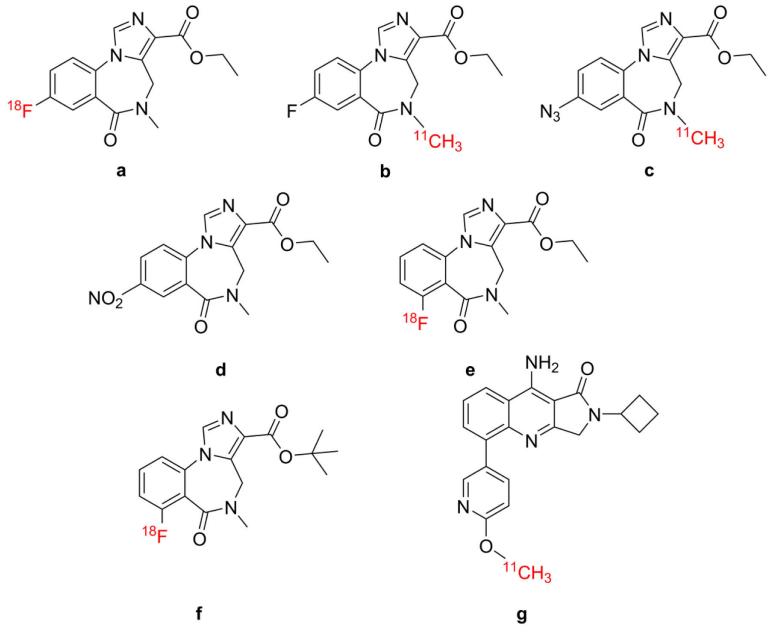


**Figure 1. Radiolabeled compounds targeting the GABA receptor**

a) [$^{18}$F]Flumazenil; b) [$^{11}$C]Flumazenil; c) [$^{18}$F]Ro15-4513; d) Nitromazenil e) [$^{18}$F]AH114726; f) [$^{18}$F]GEH120348; g) quinoline derivative developed by Moran *et al.*[15].

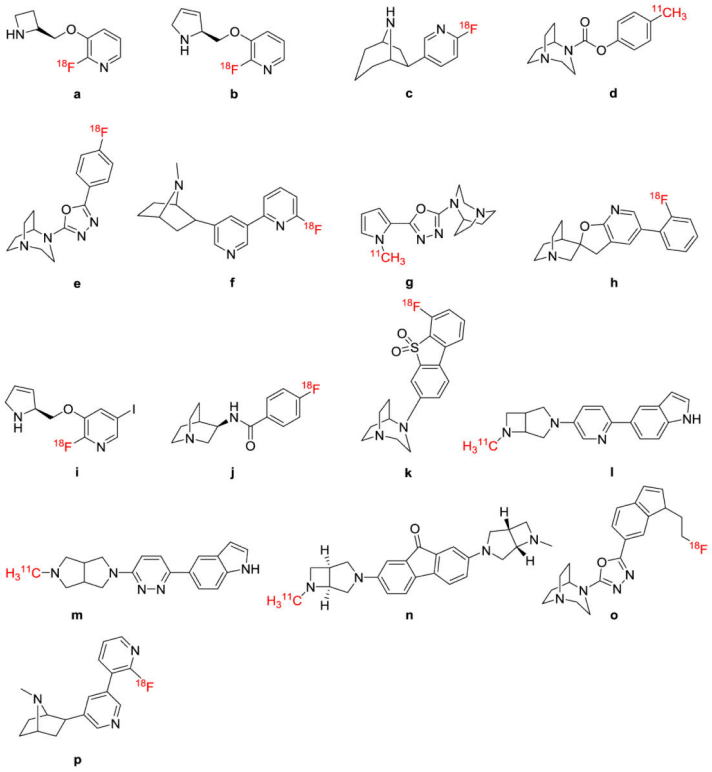


**Figure 2. Radiolabeled compounds targeting the nACh receptor**

a) [$^{18}$F]2FA; b) [$^{18}$F]Nifene; c) [$^{18}$F]Flubatine; d) [$^{11}$C]CHIBA-1001; e) [$^{18}$F]NS10743; f) [$^{18}$F]AZAN; g) [$^{11}$C]NS14492; h) [$^{18}$F]AZ11637326; i) [$^{18}$F]Niofene; j) quinuclidine derivative developed by Pin *et al.*[66]; k) [$^{18}$F]ASEM; l) [$^{11}$C]Rac-1; m) [$^{11}$C]A-833834; n) [$^{11}$C]A-752274; o) [$^{18}$F]NS14490; p) [$^{18}$F]XTRA.

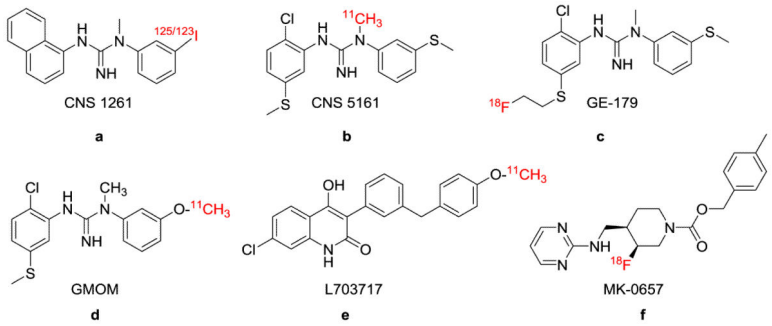


**Figure 3a. Radiolabeled compounds targeting the NMDA receptor**

a-d) ligands targeting ion channel/PCP binding site; e) ligand targeting glycine binding site and f) ligand targeting NR2B subunit.

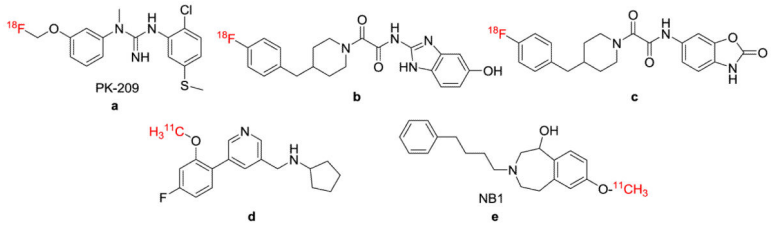


**Figure 4b.**

Recent examples in the development of NMDA imaging ligand

a-c) ligands targeting ion channel/PCP binding site; d-f) ligands targeting NR2B subunit.

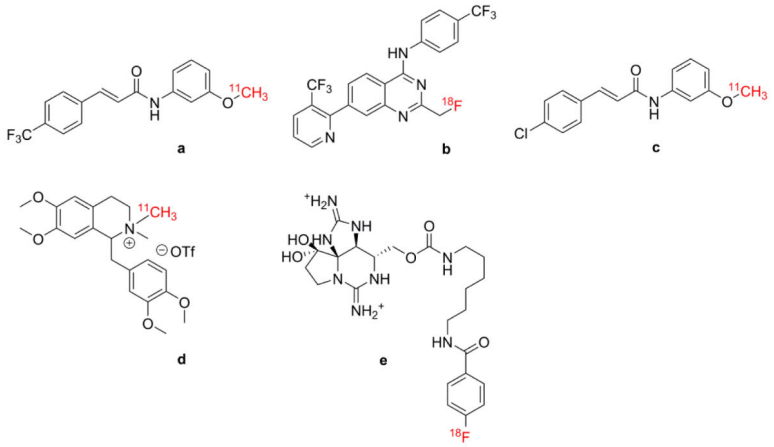


**Figure 5. Radiolabeled compounds targeting other receptor proteins**

a) [$^{11}$C]DVV24, a TRPV1 radioligand; b) [$^{18}$F]DVV54, a TRPV1 radioligand; c) [$^{11}$C]SB366791, a TRPV1 radioligand; d) a saxitoxin derivative developed by Hoehne *et al.* targeting the $Na_vs$[96]; e) tetrahydroisoquinolinium derivative developed by Gao *et al.* targeting the $SK_{Ca}$.[97]

**Table 1**

Preclinical Applications of Flumazenil and Ro15-4513

| Tracer | PET Nuclide | Animal | Reference |
|---|---|---|---|
| **Flumazenil** | [$^{18}$F] | Rhesus Monkey | 16 |
| **Flumazenil** | [$^{18}$F] | Rat | 17 |
| **Flumazenil** | [$^{11}$C] | Rhesus Monkey | 13 |
| **Flumazenil** | [$^{11}$C] | Mouse and Rat | 14 |
| **Flumazenil** | [$^{11}$C] | Rat | 12 |
| **Ro15-4513** | [$^{3}$H] | Rat | 18 |

**Table 2**

Clinical Applications of Flumazenil and Ro15-4513

| Tracer | PET Nuclide | Experimental Condition | Reference |
|---|---|---|---|
| **Flumazenil** | [$^{18}$F] | Unilateral Ischemic Stroke | 25 |
| **Flumazenil** | [$^{18}$F] | Temporal Lobe Epilepsy | 24 |
| **Flumazenil** | [$^{18}$F] | Children with Cerebral Palsy | 33 |
| **Flumazenil** | [$^{18}$F] | Ultra-High Risk for Psychosis | 26 |
| **Flumazenil** | [$^{18}$F] | Schizophrenics taking Aripiprazole | 27 |
| **Flumazenil** | [$^{18}$F] | Aversive-Aversive Stimulus | 34 |
| **Flumazenil** | [$^{18}$F] | Internal vs. External Awareness | 28 |
| **Flumazenil** | [$^{18}$F] | Healthy – Cortical Thickness | 29 |
| **Flumazenil** | [$^{11}$C] | Acute Triazolophthalazine α51A Dose | 20 |
| **Flumazenil** | [$^{11}$C] | Cerebellar Ataxia | 19 |
| **Flumazenil** | [$^{11}$C] | Epileptic Newborns | 21 |
| **Flumazenil** | [$^{11}$C] | Tiagibine GAT-1 Blockade | 22 |
| **Flumazenil** | [$^{11}$C] | Primary Distonia | 23 |
| **Ro15-4513** | [$^{11}$C] | Induced Acute GABA increase | 30 |
| **Ro15-4513** | [$^{11}$C] | History of Cigarette Smoking | 31 |
| **Ro15-4513** | [$^{11}$C] | Acute Zolpidem Dose | 32 |
| **Ro15-4513** | [$^{11}$C] | Alcohol-Dependent Men | 35 |
| **Ro15-4513** | [$^{11}$C] | Autism Spectrum Disorder | 36 |

**Table 3**

Preclinical Nicotinic Acetylcholine Receptor PET Studies

| Tracer | PET Nuclide | Animal | Reference |
|---|---|---|---|
| **Nifene** | [$^{18}$F] | Mice | 57 |
| **Nifene** | [$^{18}$F] | Rat | 58 |
| **Nifene** | [$^{18}$F] | Rat | 59 |
| **Nifene** | [$^{18}$F] | Rat | 43 |
| **Nifene** | [$^{18}$F] | Rhesus Monkey | 45 |
| **Nifene** | [$^{18}$F] | Rhesus Monkey | 44 |
| **Nifene** | [$^{18}$F] | Rhesus Monkey | 46 |
| **Flubatine** | [$^{18}$F] | Rhesus Monkey | 48 |
| **Flubatine** | [$^{18}$F] | Rhesus Monkey | 49 |
| **NS10743** | [$^{18}$F] | Pig | 60 |
| **AZAN** | [$^{18}$F] | Baboon | 61 |
| **CHIBA-1001** | [$^{11}$C] | Rat | 53 |
| **CHIBA-1001** | [$^{131}$I] | Monkey | 52 |
| **ASEM** | [$^{18}$F] | Mouse | 62 |
| **ASEM** | [$^{18}$F] | Baboon | 63 |
| **XTRA** | [$^{18}$F] | Baboon | 64 |

**Table 4**

Clinical Nicotinic Acetylcholine Receptor PET Studies

| Tracer | PET Nuclide | Experimental Condition | Reference |
|---|---|---|---|
| **2FA** | [$^{18}$F] | Neurodegenerative Disorders | 39 |
| **2FA** | [$^{18}$F] | Low Varinicline Dose, Smokers | 40 |
| **2FA** | [$^{18}$F] | Schizophrenic Smokers | 41 |
| **2FA** | [$^{18}$F] | Mild Cognitive Impairment, Alzheimer's Disease | 42 |
| **Flubatine** | [$^{18}$F] | Healthy | 50 |
| **Flubatine** | [$^{18}$F] | Alzheimer's Disease | 51 |
| **CHIBA-1001** | [$^{11}$C] | Healthy | 54 |
| **CHIBA-1001** | [$^{11}$C] | Tropisetron Dose | 55 |
| **ASEM** | [$^{18}$F] | Healthy | 65 |